RevMexAA (Serie de Conferencias), **7**, 158–162 (1998)

HST FOS SPECTROSCOPY OF ETA CARINAE'S NORTHEAST JET

T. W. Glover[1], R. J. Dufour[1], J. J. Hester [2], D. G. Currie[3], D. van Orsow[4], and D. K. Walter[5]

RESUMEN

Hemos obtenido espectros FOS en diez posiciones en la nebulosidad que rodea a η Carinae, incluyendo dos aperturas localizadas a lo largo del prominente jet que emerge hacia el noreste de la región central. A diferencia de otros espectros de η Carinae y las eyecciones que la rodean, el espectro de nuestra apertura J1 permite el cálculo de unas pocas abundancias químicas clave, libres de contaminación por luz reflejada. Esto se debe a la alta velocidad relativa a η Car del nudo de eyección contenido en esta apertura. Este espectro permite conocer cuantitativamento el impacto de la luz reflejada en las determinaciones de abundancias químicas en la nebulosa de η Carinae.

ABSTRACT

We have obtained FOS spectra of ten locations in the nebulosity surrounding η Carinae, including two apertures located along the prominent "jet" protruding northeast from the central region. Unlike previous spectra of η Carinae and its surrounding ejecta, the spectrum in our J1 aperture allows the calculation of a few key chemical abundances free of contamination by reflected light. This is due to the high velocity relative to η of the knot of ejecta contained in this aperture. This unique spectrum also yields quantitative insight into the impact of reflected light on chemical abundance determinations in the η Carinae nebula.

Key words: **ISM: INDIVIDUAL OBJECTS (ETA CARINAE) — STARS: MASS LOSS — STARS: VARIABLES: OTHER (LUMINOUS BLUE VARIABLES)**

1. INTRODUCTION

The ejecta surrounding η Carinae consists of two adjacent hollow spherical lobes with a disk-shaped equatorial "skirt" between the tangent spheres, constituting the structure described as the "homunculus" (named for its resemblance in ground-based photographs to a rotund human form). In addition to this polar-symmetric structure, a sequence of knots of ejecta (the NE jet) extends to the northeast, pointing radially outward from the central star. Another detached portion of nebulosity forms an arc cradling the Homunculus on its southwest side, the "S-condensation", in which four of our apertures lie.

It has recently been shown (Currie 1996) that portions of the nebulosity follow a Hubble-type expansion law: the tangential velocity of each part of the ejecta is directly proportional to its distance from η. This indicates that the homunculus was expelled from the central star in a single eruptive event centered on the year 1841. For the knots in our J1 and J2 apertures however, the highest-precision astrometric work done to date (Morse 1997) confirms the earlier *HST* astrometry results (Ebbetts et al. 1992), which indicated that these NE Jet features were ejected in 1860 (NN) and 1874 (NS).

Although the energy released in η Car's Great Eruption, 10^{49} ergs, exceeds by approximately a factor of ten that of the moderate eruptions of the stellar class known as the Luminous Blue Variables (LBV's), it is suspected that η's behaviour may be related to that of the LBV's. The abnormally high nitrogen abundance and circumstellar shells of η Carinae and some LBV's suggest also a connection to the Wolf-Rayet stars; recent theoretical evolution scenarios link the LBV's to WR's.

[1]Dept. of Space Physics and Astronomy, Rice University, Houston, TX 77251-1892, USA; twg@rice.edu.

[2]Dept. of Physics and Astronomy, Arizona State University, Tempe, AZ 85287, USA; rjd@rice.edu.

[3]Dept. of Physics and Astronomy, University of Maryland, College Park, MD 20742, USA.

[4]Space Telescope Science Institute, Baltimore, MD 21218, USA.

[5]Dept. of Physical Sciences, South Carolina State University, Orangeburg, SC 29117, USA.

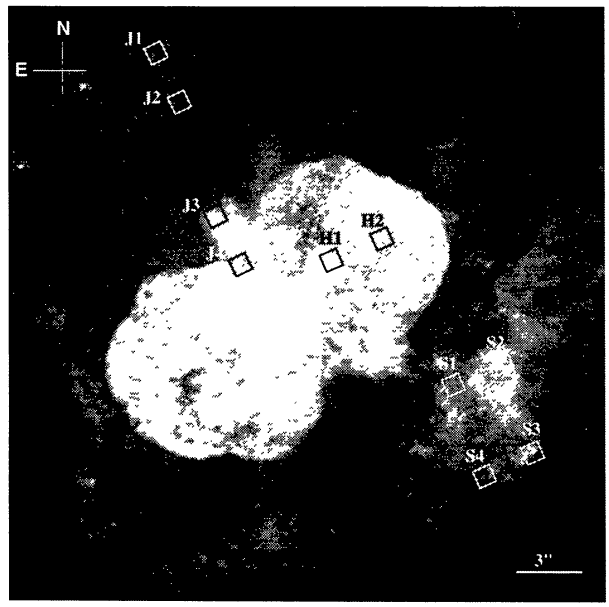

Fig. 1. The locations of our ten FOS spectra projected onto the "dithered" ultra-high-resolution *HST* WFPC2 image of the η Car nebulosities in the light of [N II] made by J. Morse et al.

2. OBSERVATIONS

The homunculus has an angular extent of $10'' \times 17''$ so that ground-based spectra of this nebulosity typically include regions of greatly differing physical, chemical and velocity characteristics, making interpretation difficult. Spectra are further complicated by the fact that the homunculus and equatorial skirt are largely dusty reflection nebulae, doppler-shifting the light from the central star by varying degrees with their complex velocity structure. Our observations were made using the paired square ($0.86''$) apertures of the *HST* FOS spectrometer. This spatial resolution allows us to examine regions of relatively uniform physical conditions and velocity, eliminating many of the obfuscations plaguing ground-based and large-aperture satellite spectra. The observations were taken during 1995 October 4 and 1996 July 4 (Cycle 5 Program GO-6042). We were able to utilize the efficiency offered by CVZ (Continuous Viewing Zone) opportunities combined with the paired-aperture capability of FOS. This enabled two sets of spectra to be obtained per offset maneuver, whereby one of the $0.86''$ apertures was placed on a primary target and the second aperture was located on a "serendipitous" position, a second target, $2.58''$ distant from the center of the primary aperture (see Table 1 and Figure 1).

3. SPECTRAL CHARACTERISTICS

Apertures J1 and J2 demonstrated far fewer lines than the apertures of the S-condensation where there is strong evidence for shocked material resulting from high-velocity bullets of material plowing through ejecta extant from earlier epochs of mass loss. We assume photoionization as the primary source of excitation for the plasma in J1 and J2. Furthermore, the velocities of these knots of ejecta result in doppler shifts which separate the inherent emission from light reflected from the central star, permitting calculation of a few ionic abundances with exceptional confidence.

J3 lies at the tip of a spade-shaped lobe apparently being ejected from the equatorial skirt. It displays a spectrum similar to that of our aperture H1, on another equatorial jet (the "paddle"). These spectra are characterized by irregular broad line profiles with relatively few collisionally excited lines, suggesting very high densities, $\approx 10^6$ cm^{-3}.

TABLE 1

HST FOS OBSERVATIONS OF ETA CARINAE EJECTA

Aper.	α(2000)	δ(2000)	Exposure Times (sec)					
			G130H	G190H	G270H	G400H	G570H	G780H
J1	$10^h45^m04.38^s$	$-59°40'52.5''$	1860	3600	1800	700	240	240
J2	04.23^s	$54.8''$	...	3600	1800	700	240	240
J3	$10^h45^m03.91^s$	$-59°40'59.4''$	900	1200	600	350	120	120
J4	03.76^s	$41'01.7''$	...	1200	600	350	120	120
H1	$10^h45^m03.30^s$	$-59°41'02.0''$	300	1200	300	146	25	43
H2	03.04^s	$00.3''$	...	1200	300	146	25	43
S2	$10^h45^m02.29^s$	$-59°41'06.6''$	1460	2400	1200	360	120	120
S1	02.55^s	$08.3''$	...	2400	1200	360	120	120
S3	$10^h45^m02.11^s$	$-59°41'10.8''$	1320	1800	900	360	120	120
S4	02.37^s	$12.5'$	...	1800	900	360	120	120

4. REDDENING

The Seaton (1979) MWG extinction law was used to correct for the effects of reddening on the emission line fluxes. $C_{H\beta}$, the logarithmic extinction at Hβ, was calculated for the Hα, Hγ, Hδ and H(9) Balmer lines, assuming Case B recombination. The separation between the peaks of the inherent and reflected lines from the dusty plasma in aperture J1 is 1.6 times the full-width at half-maximum (fwhm) of the lines, while that in J2 is 1.1 times the fwhm. The flux under each line was separated into the inherent and reflected emission by fitting two gaussians (with a common fwhm) to the line profile. In the case of J1, this permitted the calculation of separate $C_{H\beta}$'s for the two components, while the heavier overlap of the lines in J2 resulted in an uncertainty too high for meaningful results. The "model error" in the line fluxes caused by uncertainty in the velocity separation of the two components was evaluated by measuring the fluxes obtained for a range of separations equal to the variation in the splitting ($\Delta\lambda/\lambda$) of the Balmer lines. This uncertainty was ~10%, exceeding the 3% flux uncertainty attributed to instrumental error and the 1% uncertainty in flux attributed to flat-fielding. Each $C_{H\beta}$ value was weighted in proportion to the inverse of its uncertainty in calculating an average $C_{H\beta}$ for each aperture. The calculations are summarized in Table 2.

TABLE 2

LOGARITHMIC EXTINCTION AT Hβ FOR J1 HYDROGEN BALMER LINES

Component	Hα	Hγ	Hδ	H(9)	$\bar{C}_{H\beta}$
inherent	0.40±0.16	0.23±0.40	0.86±0.33	...	0.48±0.17
reflected	0.85±0.07	0.76±0.15	1.17±0.16	0.82±0.24	0.89±0.07

5. KINEMATICS OF THE NE JET

By combining astrometric determinations of the tangential velocities of the NN and NS knots with velocity information derived from our spectra, we have determined the space velocities of these knots and obtained evidence of outflow from the central object. In apertures J1 and J2, the hydrogen Balmer lines and the [N II] line at 5755 Å display consistent splitting within each aperture (see Figure 2). For J1, we find the average splitting of Hβ, Hγ, Hδ and [N II]5755 to be $\Delta\lambda/\lambda = (3.82\pm0.05) \times 10^{-3}$. In J2, [N II]5755 was weaker and omitted from the calculation, with the result for Hβ, Hγ, Hδ being $\Delta\lambda/\lambda = (3.00\pm0..09) \times 10^{-3}$.

Precise astrometric measurements of the tangential velocities of the NN and NS knots performed on the high-resolution *HST* images recently obtained by Morse are in agreement with the earlier measurements by Ebbets, with lower uncertainties. We quote their results in Table 3, with Ebbetts' results scaled from his assumed distance to η (2.8 kpc) to that assumed by Morse (2.2 kpc).

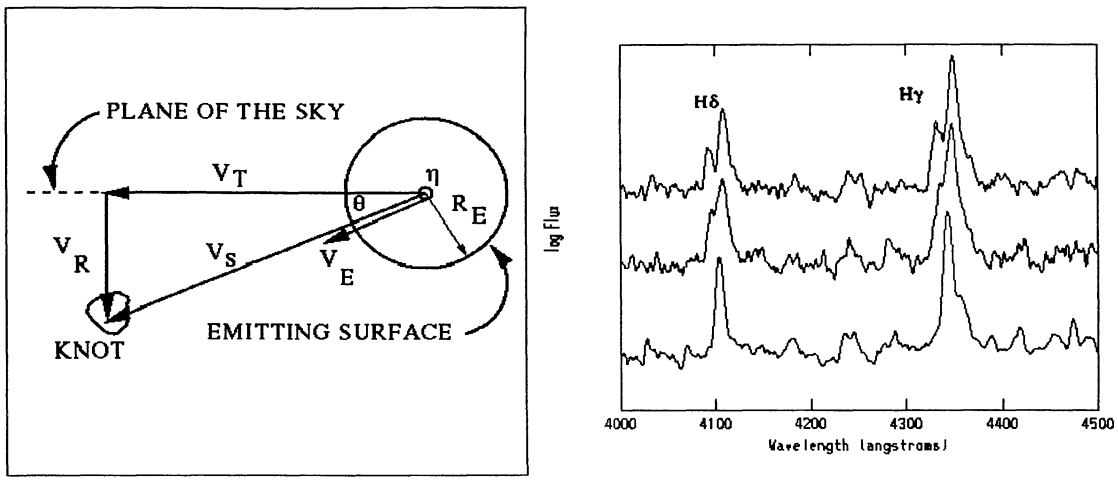

Fig. 2. (*left*) Geometry of Northeast Jet Resulting in Separation of Inherent (blue-shifted) and Reflected (red-shifted) Lines; (*right*) Top to Bottom: Apertures J1, J2, J3.

TABLE 3

NE JET ASTROMETRY RESULTS

	Morse	Ebbetts
NN v_{tan} (km s^{-1})	1016±20	1012
NN ejection date	1860±3	1862
NS v_{tan} (km s−1)	939±20	928
NS ejection date	1874±3	1870

We interpret the blue components of the split lines to be inherent emission from the knots and the (stronger) red components to be reflections of emission from the core object, η. Using the wavelength of the blue-shifted components to determine the radial velocity of each knot, we find the orientation of the knots' velocity vectors (angle out of the plane of the sky, towards the observer) to be $\theta_{NN} = 29° \pm 4°$, $\theta_{NS} = 31° \pm 4°$. If we assume that the reflected light originates from a source which is stationary, the expected line-splitting would be $(\Delta\lambda/\lambda)_{J1} = 4.20 \times 10^{-3}$ and $(\Delta\lambda/\lambda)_{J2} = 3.65 \times 10^{-3}$. This discrepancy is too large to be attributed to error in the FOS wavelength calibration. For this to be so, the systematic wavelength error in the case of J1 would have to be $\sim$ 150 km s^{-1} and for J2, the error would have to be $\sim$ 550 km s^{-1}. These "corrections" to the wavelength data would also change the orientations of the velocity vectors to 29° for NN and 0° for NS, an improbable result judging by the imagery. However, if we assume that the hydrogen line-emitting region in the core has a velocity relative to the knots V_E as indicated in Figure 2, the data for J1 and J2 yield a consistent value for this velocity: $V_{E_{NN}} = 120 \pm 60$ km s^{-1} and $V_{E_{NS}} = 200 \pm 50$ km s^{-1}. We suggest that this indicates the velocity of the outflow in the central star's hydrogen line-emitting region.

6. ELECTRON TEMPERATURE AND DENSITY

After dereddening the inherent emission line intensities with a $C_{H\beta}$ of 0.48, the [N II] ratio $(\lambda 6583 + \lambda 6548)/\lambda 5755$ yields a temperature of 9800±2600 K for the NN condensation (J1). The large uncertainty in the temperature is due to the low signal-to-noise ratio for the λ5755 line. Si III] $\lambda 1883/\lambda 1892$ yields $N_e \leq 200$ cm^{-3}.

From the stronger, red-shifted components of the split lines (the reflected light), we find $C_{H\beta} = 0.89 \pm 0.07$. Due to kinematic blending, typical density diagnostics such as the [S II] lines at 6716 Å and 6731 Å are not useful. While the 5755 Å, 6548 Å and 6583 Å [N II] lines are present, the absence of [N I] at 5200 Å and

Si III] at 1883 Å suggests a density $\geq 5 \times 10^4$. If the forbidden line emission arises from the core components studied by Davidson et al., the density may be $\sim 10^6$ cm^{-3}. Since we do not have a reliable density indicator for the reflected light, we cannot calculate abundances for its source. However, we can quantify the difference the inclusion of the reflected light makes upon the abundance calculations, and thereby get some appreciation of the significance of this effect for apertures where the kinematics does not separate the inherent and reflected flux, such as those in the S-condensation.

7. EFFECT OF REFLECTED LIGHT ON THE DETERMINATION OF CHEMICAL ABUNDANCES

With only ~30 inherent emission lines in the J1 spectrum, it is not possible to perform a complete chemical analysis of the NN knot. However, we are able to determine abundances for neutral and singly ionized nitrogen and put upper bounds on the C and O abundances. Furthermore, by combining the emitted and reflected line fluxes, we are able to quantitatively describe the impact of reflected light on the abundance calculations and emphasize the importance of taking this effect into account when considering abundances in other portions of the η Carinae nebulosity.

The error presented with each abundance (see Table 4) includes the uncertainty in the dereddened intensity (due to Poissonian noise, reddening uncertainty, flux calibration error and flat-fielding error) and the uncertainty in the electron temperature.

TABLE 4

ABUNDANCES WITH AND WITHOUT SEPARATION OF REFLECTED LIGHT

	N_e	T_e	$(N^+/H^+)_{6583}$	$(N^o/H)_{5200}$
inherent only	200	9800±2600	8.3±0.3	7.5±0.4
inherent + reflected	200	14,400±1800	7.2±0.1	6.2±0.2

The primary cause of the difference in the combined and separated light analyses is the reduction in the combined flux of the proportion of 6583 Å light due to illumination of the nebulosity in the aperture by the core region, where higher densities collisionally quench the 6583 Å emission and enhance the 5755 Å emission. This has the effect of artificially raising the [N II] temperature and thereby lowering the abundance. Since the S-condensation is also illuminated by light from the core region, we conclude that the previous estimates of the nitrogen abundance there should be considered as lower limits. Since the S-condensation surface brightness is higher than that of J1 while it is approximately the same distance from the core as J1, it is reasonable to suppose that the N^+ abundance for the S-condensation should be raised but by an amount smaller than the difference in J1, ~ 1.0 dex.

Only very weak evidence for oxygen in NN is found in an appropriately doppler-shifted line at λ3719 blended with [O II] λ3727 emission from the background H II region. From this, and an estimate for the upper limits of [O III] λ4959, λ5007, we calculate an oxygen abundance of $12 + \log[O^+/H^+] < 6.9$.

No carbon lines are discernible; upper limits for C III] λ1909 and C II] λ2326 indicate a maximum carbon abundance of ~ 7.7. The He I lines λ6678 and λ5876 indicate $[He^+/H^+] \sim 0.115 \pm 0.006$, a moderate enrichment over solar. Therefore, we conclude that, like the homunculus and the S condensations, the jet emission is from material ejected by η rather than the ambient ISM.

REFERENCES

Currie, D. G. 1996, AJ, 112, 1115
Morse, J. A. 1997, personal communication
Ebbetts, D., White, R., Walborn, N., Davidson, K., & Malumuth, E. 1992, ESO Conference and Workshop Proceedings, 44, 395
Davidson, K., Ebbetts, D., Weigelt, G., Humphreys, R., Hajian, A., Walborn, N., & Rosa, M. 1995, AJ, 109, 1784
Seaton, M. J. 1979, MNRAS, 187, 73